Nonlinear optics with ultrashort mid-infrared laser pulses

Gonçalo Alexandre Luís Vaz
goncalovaz98@tecnico.ulisboa.pt

Instituto Superior Técnico, Lisboa, Portugal

December 2021

Abstract

The rapid advances in material research over the past few years allowed the development of many new Mid-Infrared (MIR) gain materials with excellent optical and mechanical properties for the generation of ultra-short pulses, leading to the first generation of high-efficiency, low-cost, compact MIR laser systems. It is precisely one of these first-generation lasers that is now installed at the Laboratory of Intense Lasers (L2I) in Instituto Superior Técnico de Lisboa (IST), under the management of the Group of Lasers and Plasmas (GoLP), affiliated with the Instituto de Plasmas e Fusão Nuclear (IPFN).
The system is based on Optical Parametric Chirped-Pulse Amplification (OPCPA) using a laser pump of 1.03 μm generating pulses at a repetition rate of 100 kHz, each with a duration of 1 ps. The final output are 40 fs pulses delivered at 100 kHz in the 3 μm. These pulses are emitted with: an average power of 6.5 W, energy of 65 μJ, focused intensity of 2×10^{15} W/cm^2, 1.7 GW of peak power, and a Strehl ratio > 0.7. Unfortunately, due to the current pandemic, the condition of the system was sub-optimal during our experiments, and is currently being realigned by the suppliers.
This thesis reports the first set of experiments with this new state-of-the-art laser system. These experiments consisted of nonlinear spectral broadening at 1.03 μm, Supercontinuum Generation (SCG) at 3 μm, and harmonic-generation at 3 μm. Here we describe the experimental setups together with data from the laser-solid interactions. Finally, the results are compared with published data with identification of the critical parameters for high efficiency nonlinear optical interactions. **Keywords:** Harmonic generation; High-Harmonic Generation; Mid-infrared; Nonlinear optics; Supercontinuum; Spectral broadening

1. Introduction

In the past two decades, there has been a growing interest and investment in the study of ultrafast optics and ultrafast science in the Mid-Infrared (MIR), $2 - 12$ μm spectral region. This is largely due to the fact that the fundamental vibrational absorptions of most molecules reside within this range, leaving distinctive spectral fingerprints, which are of key importance for industrial, medical, and scientific applications.
During the last few years, we have witnessed the birth of the first generation of high-energy and high-efficiency laser sources in the MIR region. The introduction of such sources opened the doors to a variety of new and exciting applications, in particular in the branch of ultrafast science. Some of the most notable applications of MIR ultrafast sources are succinctly introduced in Fig.1, while a more complete review for the particular case of ultrafast laser sources operating in the $2 - 3.5$ μm is presented by Ma *et al*[1].

At the end of the year 2020, Instituto Superior Técnico de Lisboa (IST) acquired one of these new laser sources. This custom-made system is now installed in the Laboratory of Intense Lasers (L2I), a facility managed by the Group of Lasers and Plasmas (GoLP) at Instituto de Plasmas e Fusão Nuclear (IPFN) and is the first ultrashort, high-energy MIR laser system in Portugal. Not only that but this device has an output at 3 μm which, even within high-energy lasers working in the MIR, is extremely rare due to the innate inefficiency of the most gain materials at this wavelength. On top of being the first of its kind in the country, there are only a handful of similar laser systems in Europe.
The scope of this thesis is centered on exploring the capabilities of the new state-of-the-art MIR laser system installed at L2I, in particular its characterization and the development of the first series of experiments, and is divided in the following main components:

- Spectral broadening at 1.03 μm
- Supercontinuum Generation (SCG) at 3 μm
- Harmonic generation at 3 μm

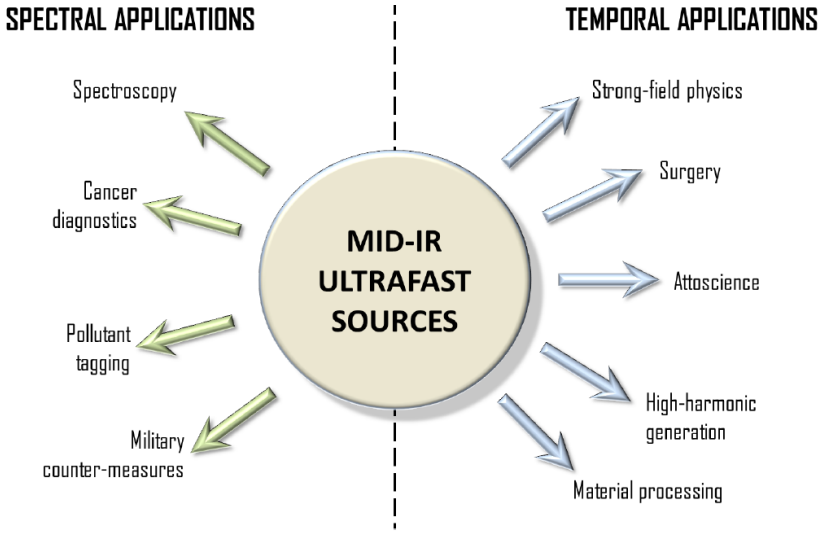

Figure 1: MIR ultrafast laser sources applications. Taken from [2]

1.1 Mid-Infrared laser systems

The rapid advances in material research over the past decade have allowed the development of many new MIR gain materials with excellent optical and mechanical properties for the generation of ultrashort pulses, leading to the first generation of high-efficiency, low cost, compact MIR laser systems. However, the presence of the vibrational modes that we want to explore leads to great losses in most materials, significantly limiting the availability of gain media and saturable absorbers for the development of laser sources. For this reason, in the early 2000s, MIR laser sources were seldom and normally extremely complex, expensive, and inefficient[1].

Even within the MIR region, the wavelengths around 3 μm can be extremely elusive. In fact, just a few years ago there were no efficient high-energy laser sources at this wavelength. For example, quantum cascade lasers at room temperature only operated properly above 3.5 μm, conventional silica fiber lasers could only generate up to 2.5 μm and many alternatives had stability and optical damage problems[3]. Today, however, there are already some efficient laser sources that are now entering the market, but naturally, these systems are still a tiny share compared with, for example, the 2 μm lasers.

The new system at IST is precisely one of these extremely rare, state-of-the-art 3 μm laser systems. Figure 2 shows the pulse energy vs. pulse duration for comparable laser systems worldwide, highlighting the parameters of the IST system.

1.2 Supercontinuum Generation

SCG has been studied extensively during the last 50 years in a multitude of nonlinear media since it was first observed by Alfano *et al*[4] in 1970. In a pioneering experiment, 5 mJ picosecond pulses at 530 nm were propagated in BK7 glass, leading to an output spectrum covering the entire visible range from 400 to 700 nm. The nonlinear broadening was not a complete novelty at the time, however, what differentiated this experiment from previous works was the extent of the generated light spectrum, being 10 times greater than anything observed before. Curiously enough their work was dedicated to the first identification of nonresonant four-photon coupling, i.e., Four-Wave Mixing (FWM) so the term ”supercontinuum” was only established in 1985 by Manassah *et al*[5].

In the following years, a variety of experiments were performed using different propagation media, mainly with nonlinear crystals and waveguides but also, on a smaller scale, air and noble gases. However, the input pulses were mainly in the visible or Near-Infrared (NIR). Only around the 2010s, we started to observe SCG based on MIR pulses, mainly due to the lack of efficient sources as mentioned.

1.3 High-Harmonic Generation

High-Harmonic Generation (HHG) in a gas medium is the oldest and most well-established way to generate high harmonics up to the extreme ultraviolet range. One of the earliest observations of HHG was made by Ferray *et al*[6] in 1988 by propagating 1064 nm, 30 fs laser pulses at 10 Hz into Ar, Kr, and Xe gases, achieving the 33^{rd}, 29^{th} and 21^{st} harmonic, respectively. An interesting property of HHG in gases is that the maximum

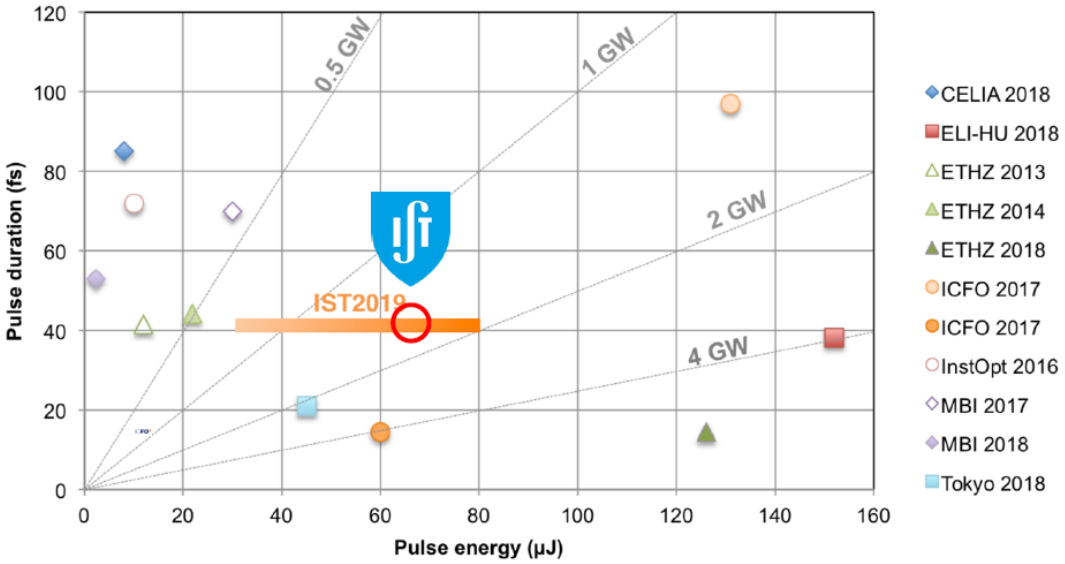

Figure 2: Laser systems ($\sim$ 3 μm, $<$ mJ) around the world.

harmonic achievable grows, approximately, with the square of the input pulse wavelength[7], which implies that (at the same level of intensity) a lower frequency laser is actually capable of achieving much higher harmonics than a higher frequency one, and thus covering a greater spectrum. Possibly, the most famous experiments of gas-based HHG, where precisely this effect can be observed, was published in 2012 by Popmintchev *et al*[8], where they guided pulses centered at a wavelength of 3.9 μm into a waveguide filled with He and achieved harmonics greater than 5000, creating a supercontinuum spanning from the MIR to the soft X-rays.

Even though HHG has been observed for over 30 years, it took over two decades to achieve it in solid media, mainly because, in solids, the harmonics generated are strongly absorbed by the material itself and are more susceptible to self-action effects (both in time and space) [9]. The first successful result was reported by Ghimire *et al*[10] in 2011 where they obtained up to the 25^{th} harmonic in a zinc oxide (ZnO) crystal injected with 3.25 μm laser pulses. The output takes the form of a train of short chirped pulses, one for each half-cycle of the input pulse. Each one of these short pulses has a spectrum in the form of a frequency comb in which the lines are separated by $2\omega_0$, where ω_0 is the input pulse central frequency. The main advantage of this technique is that we can generate extremely short pulses, down to attosecond duration, with an extremely large spectrum, in some cases thousands of harmonics, forming a supercontinuum. These pulses form the basis of attosecond science, in particular spectroscopy and imaging[11].

2. System

The laser system, Fig.3, consists of a 1.03 μm pulsed laser source that can be used directly in the experiments or as a pump of a second device, which is based on Optical Parametric Chirped-Pulse Amplification (OPCPA), to generate 3 μm pulses. A collection of the main output parameters of the two systems is presented in Tab.1.

The pump system is a *Amphos2000*, commercialized by *AMPHOS*, which is based on a diode-pump solid-state Yb:YAG resonator coupled with InnoSlab amplification[12]. The system is specified to generate pulses with a length of 0.9 – 10 ps, a repetition rate of 100 kHz, and power up to 100 W. Unfortunately, due to the current pandemic of COVID-19, and consequent traveling restrictions, this system could not be fully installed and optimized, as this procedure must be performed by *AMPHOS* technical staff. Because of this, the max output power was reduced to about 82 W and the beam was slightly elliptical, with an ellipticity of $\sim$ 0.8. This system is already under realignment by the *AMPHOS* technical team.

The system for OPCPA is a custom made *Starzz* model created by *FASTLITE*, which is based in SCG followed by multiple stages of Optical Parametric Amplification (OPA), Fig.4. This system was designed to work in a saturation regime, by receiving short pulses of 1 ps at 100 kHz with an average power of 75.5 W and an ellipticity of 1. The final output is a pulsed 3 μm beam which consists of short 40 fs pulses delivered at 100 kHz, an average power of 6.5 W, and a peak power of 1.7 GW. The beam also possesses focused inten-

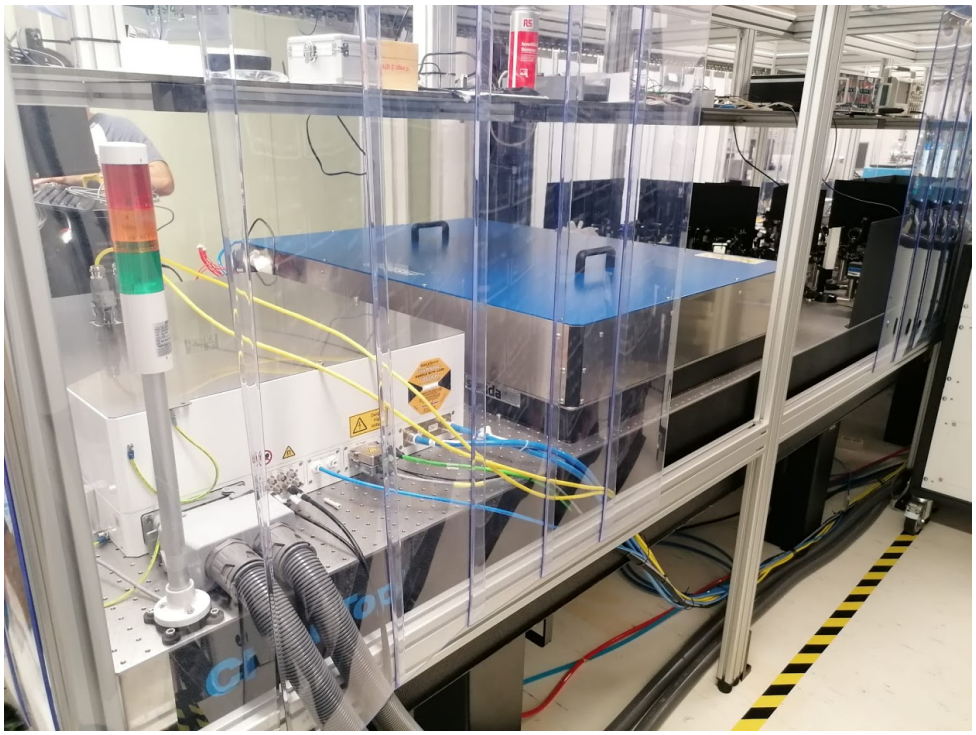

Figure 3: MIR laser system installed at L2I. The white device on the left corresponds to the 1.03 μm pump. while the blue device at the right performs the OPCPA to generate the 3 μm laser pulses.

Table 1: Specifications of the two laser systems used in this thesis.

System	Wavelength	Average Power	Repetition rate	Energy per pulse	Pulse duration
Pump by *AMPHOS*	1030 nm	100 W	100 kHz	1 mJ	1 ps
OPCPA by *FASTLITE*	3000 nm	6.5 W	100 kHz	65 μJ	40 fs

sity of 2×10^{19} W/cm^2 and a Strehl ratio > 0.7.
To perform OPCPA the pump is set to generate pulses with a repetition rate of 100 kHz and duration of 1 ps. The average power of the beam is then set to slightly above 75.5 W, this guarantees that the OPCPA system is working in a saturation regime so that any fluctuation of the pump power does not affect the 3 μm output. However, since the pump at the time was below the specified requirements, in particular the ellipticity, the average power was around 4.8 W.

3. Methodology

In this section, we present a concise description of the first set of experiments with the new laser system at L2I.

3.1 Spectral broadening at 1.03 μm

For the generation of spectral broadening, we set the pumping system to deliver short linearly polarized laser pulses with a duration of 1 ps, at a repetition rate of 100 kHz and a maximum average power of 82 W. These pulses were focused with a focal lens into a sample placed slightly after the focus, as to prevent optical damage and to counteract the self-focusing that the laser beam might experience due to Kerr effects[13]. The beam was then sent to a wedge that reflected $\sim$ 10% of the beam to seven absorptive filters that reduce the power of the beam to avoid damaging the remaining components. After the filters, the beam entered an integrating sphere, which was connected by an optical fiber to a spectrometer. The effect of the transmission of the filters was corrected using the data given by the manufacturers.
We started by placing a fused silica sample (5 mm thick) far away from focus and measured the spectrum at the output. This allowed us to study the dependence of the broadening with the input power, in particular the value of Full width at half maximum (FWHM). This procedure was repeated two more times, as we placed the sample closer to focus until we observed the formation of optical damage. After this, all other samples were placed in the position before the optical damage was observed and the same procedure was repeated. These samples consisted of: CaF_2 (1 mm), sapphire (15 mm), and YAG (4 mm). In this wavelength, all samples are in the normal dispersion regime.
Numerical simulations were performed using an

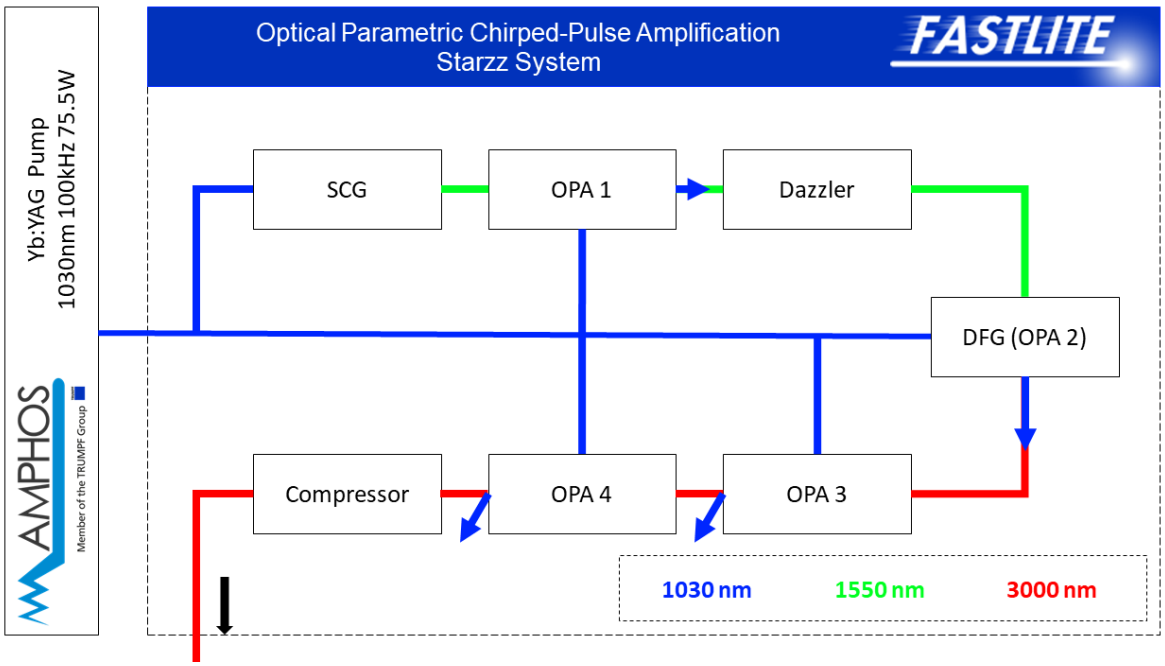

Figure 4: Schematic of the 3 μm laser system. The second stage of OPA is phase-matched to generate a frequency equal to the difference of the two input beams, e.g.Difference-Frequency Generation (DFG). As or the *Dazzler*, it is a *FASTLITE* tool for compression optimization and Carrier-Envelope Phase (CEP) stabilization.

open-source code: pyNLO[1]. Which is based on solving the Generalized Nonlinear Schrödinger Equation (GNLSE)[14] for an optical fiber, in our case an "equivalent" optical fiber that represents our samples. This kind of approach has been previously used for the simulation of spectral broadening in a Multipass cell[15]. The simulations were adjusted to approach the experimental results so that by comparison we could propose a hypothesis of the interactions and dynamics leading to this spectral broadening, in particular the transverse area of the laser beam. To calculate this area we first had to calculate the beam parameters of the laser. For this, we used the data from a set of measurements used for planing a future setup on the lab, which included the propagation of the beam through a telescope (for resizing) into a camera moved along the propagation path. This data was then fitted to the expression for a perfect Gaussian beam[13] and traced back to the laser, for recovery of the output parameters, and then propagated through our experimental setup using a software for simulation of optical systems.

3.2 Supercontinuum Generation at 3 μm

The generation of supercontinuum at 3 μm is the result of a "failed" attempt to acquire harmonics where the continuum masked the harmonic signal. We propagated short linearly polarized pulses of 40 fs at a repetition rate of 100 kHz into a focal lens, which then sends the beam to the samples. During the generation of harmonics, we used two different experimental setups: one where we used a wedge to send to the sample just $\sim$ 0.48 W in a tight focus; another where the wedge was replaced by a silver mirror to send 4.8 W with a soft focus to avoid damaging the samples. In the low-power setup, the samples were placed at focus, while in the high-power setup the samples had to be placed after the focus, once again to avoid damage. After the samples, the beam was collimated into a dispersion prism to separate the different components of the spectrum into an integrating sphere. The fundamental wavelength was blocked by a beam dump to avoid damaging the optical fiber connected to this sphere, which then transfers the signal to a spectrometer. The spectrometer is a standard system based in Si with a spectral range of 147 – 1127 nm. Unfortunately, this does not include the entirety of the supercontinuum, for that we would need to also measure the spectrum with a MIR spectrometer and possibly a Ultraviolet (UV) spectrometer, which can be rather expensive. The samples that generated supercontinuum were CaF_2 (3 mm), fused silica (5 mm), sapphire (1 mm), and YAG (1, 2 and 4 mm). In this wavelength, all samples are in the anomalous dispersion regime.

[1] pyNLO-Nonlinear optics modeling for Python: https://pynlo.readthedocs.io/en/latest/readme_link.html and https://github.com/pyNLO/PyNLO, Version 0.1.2

3.3 Harmonic generation at 3 μm

The setup for harmonic generation is the same as described in the previous section with the exception that instead of an integrating sphere the optical fiber is mounted on a translator, to collect each harmonic individually, and send them to a spectrometer. By moving this translator we searched for any individual harmonics with the spectrometer. When we located a harmonic we used the rotation mount to rotate the samples around their axis and the spectrum was taken in intervals, in most cases of 10º, until covering the entire 360º. The process was then repeated for each available harmonic and the sample was switched. The samples used in these experiments were: CaF_2 (1 mm and 3 mm), fused silica (5 mm), LiF (3 mm), and sapphire (1 mm and 2 mm). For many samples, it was possible to obtain harmonics in both setups. In the case of the LiF sample, we also were able to obtain harmonics in multiple positions due to its large band-gap that reduced the chances of generating optical damage.

For each harmonic, the number of counts obtained in the spectrometer, $C(\lambda)$, was fitted to a Gaussian function to obtain the normalization constant, C_0. As C_0 is proportional to the energy of the harmonic, we studied the effect of the polarization on the efficiency of the generation process. To verify the accuracy of this fit we also present the similar study using instead for area beneath the harmonic defined as $\int_{\lambda_1}^{\lambda_2} C(\lambda)\, d\lambda$, where λ_1 and λ_2 are, respectively, the lowest and the highest wavelength in which $C(\lambda_{1,2}) = \max\{C(\lambda)\}/e^2$, $\lambda_2 > \lambda_1$.

In the LiF and the two sapphires samples, we noticed that the 3rd harmonic spectra presented an interference pattern. This pattern was consistent with the one observed in Third Harmonic Generation (THG) by Garejev *et al*[16] in a CaF_2 sample. They observed that this interference was a result of the formation of two different components of the third harmonic near the surface o the sample. While one of them traveled at the group velocity associated with its wavelength (free component) the other traveled together with the remaining pulse (driven component). This group velocity mismatch resulted in the temporal separation of the two components and hence the interference pattern in the spectrum. To test this possibility we performed an Inverse Fourier Transform (IFT) of the spectra to measure the temporal separation between the two components and compared it to the value predicted by theory.

Finally, we used a supercontinuum spectrum created by a 4 mm YAG sample and measured the resulting power. The fiber was then placed in different positions to recover multiple spectra which then were used to reconstruct the full supercontinuum. This allowed us to define a proportionality between the rate of counts from the spectrometer and the associated power. With this, we calculated both the power and power conversion efficiency of each of the harmonics obtained. As the supercontinuum was too strong to measure each point in the same conditions we had to place a filter in front of the integrating sphere. But as the power after the filter was too low to measure we once again had to reconstruct the spectra using the transmission data from the manufacturers.

4. Results and discussion

Here we present the main results from our experiments together with a short discussion of the physical principles behind them.

4.1 Spectral broadening at 1.03 μm

In all samples, we observed an increase of FWHM with the input power, a clear signal of nonlinear broadening. Additionally, as the power increases the spectra become asymmetric with an accentuated growth in the lower wavelengths/higher frequencies, which is associated with the nonlinear effect: self-steepening[13].

From the change of the position of the fused silica sample, we observed a sharp increase of the broadening as the sample got closer to focus, due to the increase of the intensity, until the formation of optical damage that caused a sharp drop in the value of FWHM. We also observed the strong dependence with the propagation length, as a 1 mm CaF_2 sample generated less broadening (FWHM= 2.6 nm) at 70% of the maximum laser output than the 15 mm sapphire sample (FWHM= 3.2 nm) at a mere 25%. In Fig.5 is represented the larger broadening obtained, in this regime, where we used the fused silica sample.

It was not possible to precisely replicate the experimental results through simulations (e.g Fig.6)

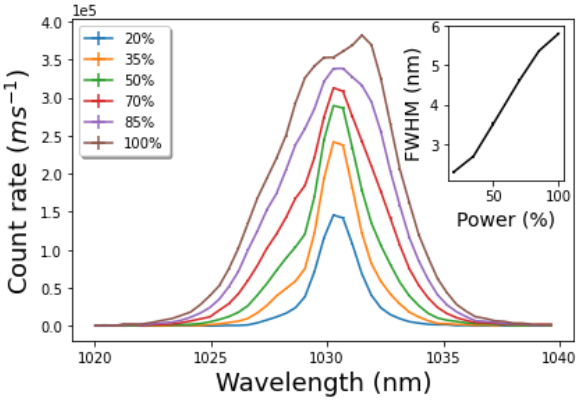

Figure 5: Spectral broadening at 1.03 μm with a fused silica sample placed 45 cm away from the focal lens. The captions are the percentage of the full power (82 W) sent to the sample. The inset depicts the variation of FWHM with the power.

as they did not include the effects of self-focus and filamentation. However, through the comparison of the simulated beam transverse area with the experimental caustic, we could conclude that, for many cases, the beam self-focused inside the media. Additionally, we observed that the asymmetry was far too great to be a result of Kerr effects only. A possibility is that after self-focusing the intensity was enough to generate free electrons that contribute to a stronger self-steepening by increasing the group velocity of the trailing part of the pulse[17]. This points to the formation of filaments inside of our samples, which in the case of fused silica is supported by the observation of segmented optical damage associated with the filament's hot-spots.

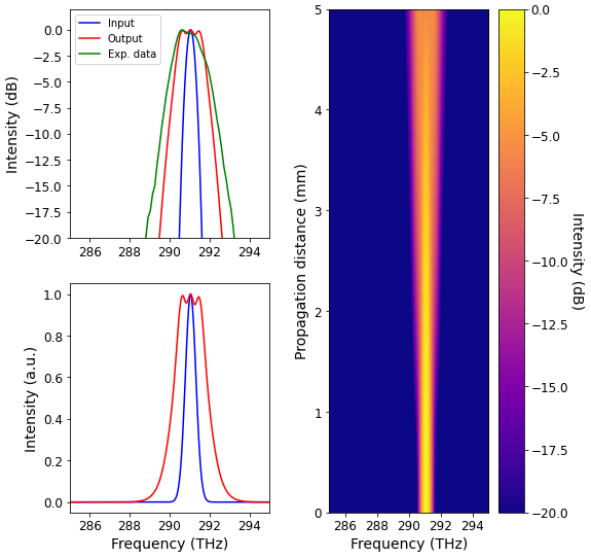

Figure 6: Simulation of the spectral broadening observed in Fig.5, at 100% of the input power. On the left is the comparison of the numerical input and output pulse together with the experimental data. On the right is the numerical spectral variation with propagation. The curves were truncated at –20 dB.

4.2 Supercontinuum Generation at 3 μm

For all samples, we observed the formation of spectral wings near the visible range, see e.g. Fig.7. This observation is in agreement with previous experimental works in the anomalous dispersion regime using MIR sources up to 2.5 μm[18, 19, 20]. In particular, the spectra of CaF_2 and fused silica which present a similar shape to the ones observed in [18] with an input laser field at 2.2 μm. These isolated wings are normally associated with the superposition light waves that were scattered by the polarization waves[19], caused by the passage of the pulse.

In this experiment, we also observed conics emission[17] associated with a filamentation regime, see e.g. Fig.7.

4.3 Harmonic generation at 3 μm

Overall, the dependency of the 3rd harmonics with polarization matches what is observed in literature for perturbative harmonics, associated with a nonlinear susceptibility e.g.THG. With the exception of a sapphire sample that was then associated with a mislabeling of the type of cut, see e.g. Fig.8. The power conversion efficiency also matched the observation of perturbative harmonics up to the 5th order. However, in the particular case of 1 mm CaF_2 sample, where we reached up to the 9th harmonic, while there is a possibility that this result is perturbative, we could not exclude beyond reasonable doubt that it could result from HHG.

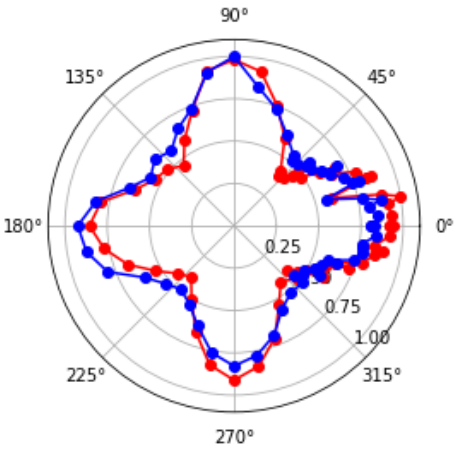

Figure 8: Dependency of the third harmonic intensity with the polarization in a 1 mm sapphire sample, unknown cut.The radius corresponds to the normalized area beneath the curve obtained in the spectrometer. In red calculated by a Gaussian fit and in blue by a numerical integration within 1/e^2 of the maximum number of counts.

The results obtained from the Fourier analysis of the interference patterns of the 3rd harmonic showed a remarkable agreement with the theoretical values, see e.g. Fig.9. In addition, we could justify the absence of these interference patterns for the other samples. In the case, CaF_2 the phase and group velocity mismatches were smaller than in the other samples and the ones observed by Garjev *et al*[16]. As for fused silica, this sample would lead to a larger temporal separation and hence an interference pattern with many peaks extremely close to each other, and it is possible that our spectrometer did not possess the necessary resolution to discern between consecutive peaks.

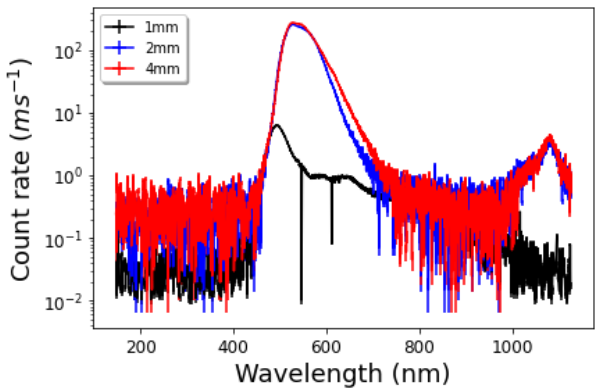

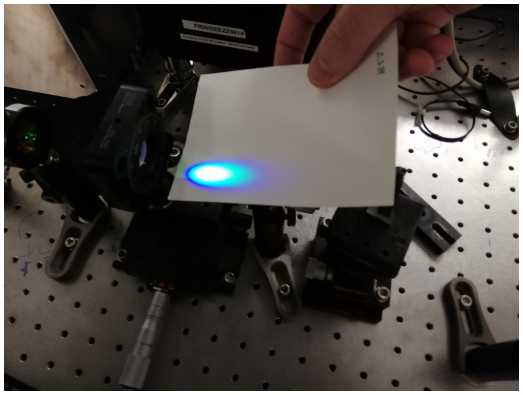

Figure 7: SCG at 3 μm with YAG samples placed at focus. On the left the spectra of the observed spectral wings, where the captions represent the thickness of the sample. On the right the resulting conical emission observed with the 4 mm sample, note the white-light at the center of the beam (supercontinuum) surrounded by the scattered frequencies.

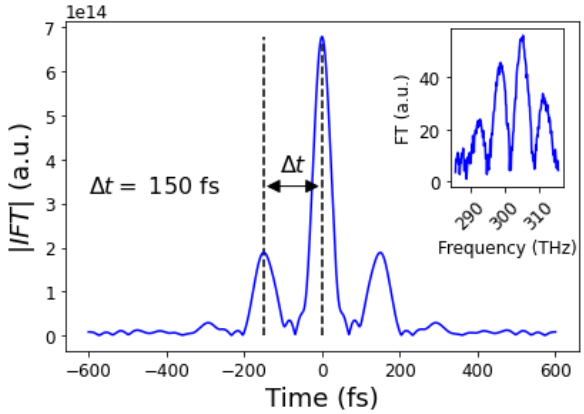

Figure 9: Absolute value of the IFT for the THG spectra, in the inset the supposed Fourier Transform (FT) using one of the spectra obtained with a LiF sample. The theoretical predicted value for Δt is 148 fs.

5. Conclusions

In the work reported in this thesis we explored some of the capabilities of the new laser system installed at L2I in the IST Alameda campus. This section makes a quick review of the main topics and results of this thesis together with some possibilities for future works.

5.1 Spectral broadening

We performed spectral broadening in the normal (1.03 μm) and anomalous (3 μm) dispersion regime, the last leading to the formation of a supercontinuum.

For the normal regime, we experimentally observe the importance of the intensity and propagation length for the broadening. The experimental data was then compared to a simplified theoretical model, based on solving a GNLSE in a nonlinear waveguide but in the absence of self-focus or filamentation. The miss-match between the experiment and this model points to the formation of a filament in the samples, due to self-focusing, with the formation of free electrons.

In the anomalous regime, we have observed the wings of the supercontinuum which includes the visible range, this is in agreement with other experimental works. The spectral broadening achieved is many times larger than what we achieved using the 1.03 μm pump even if the pump power is $\sim$ 17 times higher than the 3 μm laser, going from a FWHM= 6 nm to the formation of wings more than 2000 nm away from the fundamental. This is proof of the advantages of the new system at L2I that now allows us to observe these new and exotic physical phenomena.

An interesting study at 3 μm would be the study of the full supercontinuum spectra instead of only the wings. We currently possess a *MOZZA* spectrometer by *FASTLITE* with a spectral range of 1 – 5 μm which, together with the spectrometer used in our experiments (*FLEX-STD-UV-Vis-NIR*, *SARSPEC*) would allow us to cover the entire supercontinuum spectrum. During our experiments, we had some coupling problems with this system, and as such were unable to use it, but once these problems are fixed we should be able to obtain the desired data. Another component to study would be the variation of the temporal shape of the pulses in both sets of experiments, this would allow studying the possibility of pulse-splitting or self-compression. A possible way to do this would be using a Frequency-Resolved Optical Gating (FROG) system. In fact, in parallel to this thesis, there was the development of such a system designed for $\sim$ 3 μm, as we already possessed such a system for the $\sim$ 1 μm.

5.2 Harmonic generation

We also demonstrated harmonic generation from a 3 μm laser field, where we study the dependence of the efficiency with the orientation of the polarization in a variety of media and harmonic orders. Which, overall, coincide with the expected results from perturbative harmonic generation.

Additionally, we performed Fourier analysis of some of the obtained THG spectra that presented an interference pattern. This study points to the formation of two THG components: free and driven. The results are within the predicted by theory[16], including the lack of observation of these two components in other samples.
After this, we perform a study of the power efficiency of the harmonic generation which is once again within expectations for perturbative harmonic generation, at least for the 3^{rd} and 5^{th} harmonic.
The generation of harmonics, in particular, HHG normally involves custom-made thin crystals of the order of microns, while our samples are all thicker than 1 mm and many times are doped, as they are standardized samples. So one of the next steps to obtain HHG would be to acquire such crystals. In that sense, we would also need means to more accurately control the energy sent to the samples, which could imply the acquisition of a half-wave plate and a polarizer for the 3 μm range. This is of particular importance to study the dependency on the intensity of the harmonics with the fundamental electric field to discern between perturbative harmonic generation and HHG.
Additionally, while our Fourier approach produced good results it might be preferable to measure directly the temporal shape of the third-harmonics. This could be accomplished, once again, with a FROG system, in this case the ~ 1 μm.
Finally, all the harmonic spectra were taken while changing the sample's orientation manually. Even in the cases where we measured in intervals of 10º (the largest interval used but in some cases, we used intervals of 4º) that would result in 36 acquisitions, which amounts, for our 25 presented harmonics, to least 900 acquisitions. So naturally, it would be preferable to automatize the system to acquire more data and with higher accuracy. The same idea can also be applied to the position of the sample that is controlled manually using the translation stage. In that regard, we are in the process of acquiring motorized equipment to automatize the entire process for future experiments, either by us or other groups within GoLP or other partnerships.

References

[1] J. Ma, Z. Qin, G. Xie, L. Qian, and D. Tang, "Review of mid-infrared mode-locked laser sources in the 2.0 μ m–3.5 μ m spectral region," *Applied Physics Reviews*, vol. 6, no. 2, p. 021317, jun 2019. [Online]. Available: http://aip.scitation.org/doi/10.1063/1.5037274

[2] H. Pires, M. Baudisch, D. Sanchez, M. Hemmer, and J. Biegert, "Ultrashort pulse generation in the mid-IR," *Progress in Quantum Electronics*, vol. 43, pp. 1–30, sep 2015. [Online]. Available: https://linkinghub.elsevier.com/retrieve/pii/S0079672715000312

[3] M. R. Abu Hassan, F. Yu, W. J. Wadsworth, and J. C. Knight, "Cavity-based mid-IR fiber gas laser pumped by a diode laser," *Optica*, vol. 3, no. 3, p. 218, mar 2016. [Online]. Available: https://www.osapublishing.org/abstract.cfm?URI=optica-3-3-218

[4] R. R. Alfano and S. L. Shapiro, "Emission in the region 4000 to 7000 Å via four-photon coupling in glass," *Physical Review Letters*, vol. 24, no. 11, pp. 584–587, mar 1970. [Online]. Available: https://link.aps.org/doi/10.1103/PhysRevLett.24.584

[5] J. T. Manassah, R. R. Alfano, and M. Mustafa, "Spectral distribution of an ultrafast supercontinuum laser source," *Physics Letters A*, vol. 107, no. 7, pp. 305–309, feb 1985. [Online]. Available: https://linkinghub.elsevier.com/retrieve/pii/0375960185906413

[6] M. Ferray, A. L'Huillier, X. F. Li, L. A. Lompre, G. Mainfray, and C. Manus, "Multiple-harmonic conversion of 1064 nm radiation in rare gases," *Journal of Physics B: Atomic, Molecular and Optical Physics*, vol. 21, no. 3, pp. L31–L35, feb 1988. [Online]. Available: https://iopscience.iop.org/article/10.1088/0953-4075/21/3/001

[7] B. E. A. Saleh and M. C. Teich, *Fundamentals of Photonics*, 3rd ed. Wiley Blackwell, 2019.

[8] T. Popmintchev, M. C. Chen, D. Popmintchev, P. Arpin, S. Brown, S. Ališauskas, G. Andriukaitis, T. Balčiunas, O. D. Mücke, A. Pugzlys, A. Baltuška, B. Shim, S. E. Schrauth, A. Gaeta, C. Hernández-García, L. Plaja, A. Becker, A. Jaron-Becker, M. M. Murnane, and H. C. Kapteyn, "Bright coherent ultrahigh harmonics in the keV x-ray regime from mid-infrared femtosecond lasers," *Science*, vol. 336, no. 6086, pp. 1287–1291, jun 2012. [Online]. Available: https://www.sciencemag.org/lookup/doi/10.1126/science.1218497

[9] G. Vampa, Y. S. You, H. Liu, S. Ghimire, and D. A. Reis, "Observation of backward high-harmonic emission from solids," *Optics Express*, vol. 26, no. 9, p. 12210, apr 2018. [Online]. Available: https://www.osapublishing.org/abstract.cfm?URI=oe-26-9-12210

[10] S. Ghimire, A. D. DiChiara, E. Sistrunk, P. Agostini, L. F. DiMauro, and D. A. Reis, "Observation of high-order harmonic generation in a bulk crystal," *Nature Physics*, vol. 7, no. 2, pp. 138–141, feb 2011. [Online]. Available: http://www.nature.com/articles/nphys1847

[11] F. Calegari, G. Sansone, S. Stagira, C. Vozzi, and M. Nisoli, "Advances in attosecond science," *Journal of Physics B: Atomic, Molecular and Optical Physics*, vol. 49, no. 6, p. 062001, mar 2016. [Online]. Available: http://dx.doi.org/10.1088/0953-4075/49/6/062001https://iopscience.iop.org/article/10.1088/0953-4075/49/6/062001

[12] P. Russbueldt, D. Hoffmann, M. Hofer, J. Lohring, J. Luttmann, A. Meissner, J. Weitenberg, M. Traub, T. Sartorius, D. Esser, R. Wester, P. Loosen, and R. Poprawe, "Innoslab amplifiers," *IEEE Journal of Selected Topics in Quantum Electronics*, vol. 21, no. 1, pp. 447–463, jan 2015. [Online]. Available: http://ieeexplore.ieee.org/document/6843864/

[13] P. Rüdiger, *Encyclopedia of laser physics and technology*, 1st ed. Wiley-VCH, 2008, accessed online version on 10-2021. [Online]. Available: https://www.rp-photonics.com/encyclopedia.html

[14] J. Hult, "A fourth-order Runge–Kutta in the interaction picture method for simulating supercontinuum generation in optical fibers," *Journal of Lightwave Technology*, vol. 25, no. 12, pp. 3770–3775, dec 2007. [Online]. Available: http://ieeexplore.ieee.org/document/4397001/

[15] N. Daher, F. Guichard, S. W. Jolly, X. Délen, F. Quéré, M. Hanna, and P. Georges, "Multipass cells: 1D numerical model and investigation of spatio-spectral couplings at high nonlinearity," *Journal of the Optical Society of America B*, vol. 37, no. 4, p. 993, apr 2020. [Online]. Available: https://www.osapublishing.org/abstract.cfm?URI=josab-37-4-993

[16] N. Garejev, I. Gražulevičiūtė, D. Majus, G. Tamošauskas, V. Jukna, A. Couairon, and A. Dubietis, "Third- and fifth-harmonic generation in transparent solids with few-optical-cycle midinfrared pulses," *Physical Review A*, vol. 89, no. 3, p. 033846, mar 2014. [Online]. Available: https://link.aps.org/doi/10.1103/PhysRevA.89.033846

[17] S. L. Chin, S. A. Hosseini, W. Liu, Q. Luo, F. Théberge, N. Aközbek, A. Becker, V. P. Kandidov, O. G. Kosareva, and H. Schroeder, "The propagation of powerful femtosecond laser pulses in opticalmedia: physics, applications, and new challenges," *Canadian Journal of Physics*, vol. 83, no. 9, pp. 863–905, sep 2005. [Online]. Available: http://www.nrcresearchpress.com/doi/10.1139/p05-048

[18] J. A. Dharmadhikari, R. A. Deshpande, A. Nath, K. Dota, D. Mathur, and A. K. Dharmadhikari, "Effect of group velocity dispersion on supercontinuum generation and filamentation in transparent solids," *Applied Physics B*, vol. 117, no. 1, pp. 471–479, oct 2014. [Online]. Available: http://link.springer.com/10.1007/s00340-014-5857-3

[19] M. Durand, K. Lim, V. Jukna, E. McKee, M. Baudelet, A. Houard, M. Richardson, A. Mysyrowicz, and A. Couairon, "Blueshifted continuum peaks from filamentation in the anomalous dispersion regime," *Physical Review A*, vol. 87, no. 4, p. 043820, apr 2013. [Online]. Available: https://link.aps.org/doi/10.1103/PhysRevA.87.043820

[20] E. O. Smetanina, V. O. Kompanets, S. V. Chekalin, A. E. Dormidonov, and V. P. Kandidov, "Anti-Stokes wing of femtosecond laser filament supercontinuum in fused silica," *Optics Letters*, vol. 38, no. 1, p. 16, jan 2013. [Online]. Available: https://www.osapublishing.org/abstract.cfm?URI=ol-38-1-16